Charge order lock-in by electron-phonon coupling in La<inf>1.675</inf>Eu<inf>0.2</inf>Sr<inf>0.125</inf>CuO<inf>4</inf>

CONDENSED MATTER PHYSICS

Charge order lock-in by electron-phonon coupling in $La_{1.675}Eu_{0.2}Sr_{0.125}CuO_4$

Qisi Wang[1]*†, Karin von Arx[1,2†], Masafumi Horio[1], Deepak John Mukkattukavil[3], Julia Küspert[1], Yasmine Sassa[2], Thorsten Schmitt[4], Abhishek Nag[5], Sunseng Pyon[6], Tomohiro Takayama[7], Hidenori Takagi[8], Mirian Garcia-Fernandez[5], Ke-Jin Zhou[5], Johan Chang[1]*

Charge order is universal to all hole-doped cuprates. Yet, the driving interactions remain an unsolved problem. Electron-electron interaction is widely believed to be essential, whereas the role of electron-phonon interaction is unclear. We report an ultrahigh-resolution resonant inelastic x-ray scattering (RIXS) study of the in-plane bond-stretching phonon mode in stripe-ordered cuprate $La_{1.675}Eu_{0.2}Sr_{0.125}CuO_4$. Phonon softening and lifetime shortening are found around the charge ordering wave vector. In addition to these self-energy effects, the electron-phonon coupling is probed by its proportionality to the RIXS cross section. We find an enhancement of the electron-phonon coupling around the charge-stripe ordering wave vector upon cooling into the low-temperature tetragonal structure phase. These results suggest that, in addition to electronic correlations, electron-phonon coupling contributes substantially to the emergence of long-range charge-stripe order in cuprates.

INTRODUCTION

The ubiquity of charge order in hole-doped cuprates has motivated the investigation of its underlying mechanism (*1*). This task is complicated by the fact that charge, spin, and lattice degrees of freedom are intimately coupled in the presence of strong correlations. Prevalent theories suggest that charge order in underdoped cuprates develops predominantly from strong electronic interactions (*2*–*5*). The competition between magnetic and kinetic energies drives the tendency of doped holes toward clustering into charged stripes—often dubbed stripe order. This is in contrast to the scenario where charge density wave (CDW) order emerges due to momentum-dependent electron-phonon coupling (EPC) (*6*–*8*). These two mechanisms for charge ordering are difficult to differentiate since (i) charge modulation in both cases couples to the underlying lattice and (ii) it is difficult to evaluate the EPC and its reciprocal space variation. From hereon, CDW order refers broadly to a static charge modulation irrespective of the driving mechanism, which is the topic of this article.

Phonon anomalies in vicinity to the CDW ordering wave vector suggest the importance of electron-phonon interaction (*9*, *10*). It has, however, been difficult to extract the EPC strength, let alone its momentum dependence. Inelastic neutron and x-ray scattering (INS and IXS) (*9*, *10*) or angle-resolved photoemission spectroscopy self-energy studies (*11*, *12*) infer the EPC strength based on the assumption of bare phononic or electronic dispersions. Typically, the experimentally extracted self-energies based on these assumptions are not sensitive to subtle crystalline structural changes. Yet, in underdoped cuprates, charge order seems to be favored by certain crystal structures. For example, the low-temperature tetragonal (LTT) structure appears as the ideal host for the CDW order (*2*, *13*, *14*). This leads to the perception that the LTT phase enhances the coupling to the electronic stripes (*2*, *15*). It has, however, not been possible to experimentally establish any relation between the specific crystal structures and electron-phonon interaction.

Recent advances of the resonant IXS (RIXS) technique have enabled studies of optical phonons, charge excitations, and their Fano interference (*16*–*22*). The RIXS phonon scattering cross section is directly proportional to the EPC strength (see Fig. 1, A and B) (*16*, *23*–*27*). It is therefore possible to study both the self-energy effects (excitation energy shift and lifetime) and the EPC strength for specific phonon modes.

Here, we use ultrahigh-energy-resolution RIXS to address the EPC in the stripe-ordered compound $La_{1.675}Eu_{0.2}Sr_{0.125}CuO_4$ (LESCO). We show how the EPC is enhanced upon cooling from the low-temperature orthorhombic into the LTT phase that boosts the CDW order. Specifically, we study the in-plane copper-oxygen bond-stretching phonon mode as a function of temperature and momentum. A phonon softening anomaly in vicinity to the CDW ordering wave vector is found to persist beyond the LTT phase. In the same momentum range, we find that the EPC strength is enhanced upon cooling into the LTT phase. The enhanced EPC shows a strong momentum dependence, peaking near the charge ordering wave vector. While the phonon anomaly corresponds to an energy softening of less than 10%, the EPC is enhanced by about 20% in the LTT phase. Our results suggest that the enhanced EPC amplifies the CDW order. Both electronic correlations and momentum-dependent EPC are responsible for the charge ordering in this cuprate compound. While fluctuating stripes emerge spontaneously from strong electronic interactions at high temperature, they are stabilized at low temperature via the enhanced coupling to the host lattice.

RESULTS

A RIXS spectrum obtained at $\mathbf{Q}$ = (0.43, 0.03) (Fig. 1C) reveals a pronounced excitation around 60 meV that dominates over elastic scattering and the paramagnon excitations. We assign this excitation to the in-plane copper-oxygen bond-stretching phonon (see Fig. 1B),

[1]Physik-Institut, Universität Zürich, Winterthurerstrasse 190, CH-8057 Zürich, Switzerland. [2]Department of Physics, Chalmers University of Technology, SE-412 96 Göteborg, Sweden. [3]Department of Physics and Astronomy, Uppsala University, Box 516, SE-751 20 Uppsala, Sweden. [4]Swiss Light Source, Photon Science Division, Paul Scherrer Institut, CH-5232 Villigen PSI, Switzerland. [5]Diamond Light Source, Harwell Campus, Didcot, Oxfordshire OX11 0DE, UK. [6]Department of Applied Physics, The University of Tokyo, Tokyo 113-8656, Japan. [7]Max Planck Institute for Solid State Research, 70569 Stuttgart, Germany. [8]Department of Physics, The University of Tokyo, Tokyo 113-0033, Japan.
*Corresponding author. Email: qisiwang@physik.uzh.ch (Q.W.); johan.chang@physik.uzh.ch (J.C.)
†These authors contributed equally to this work.

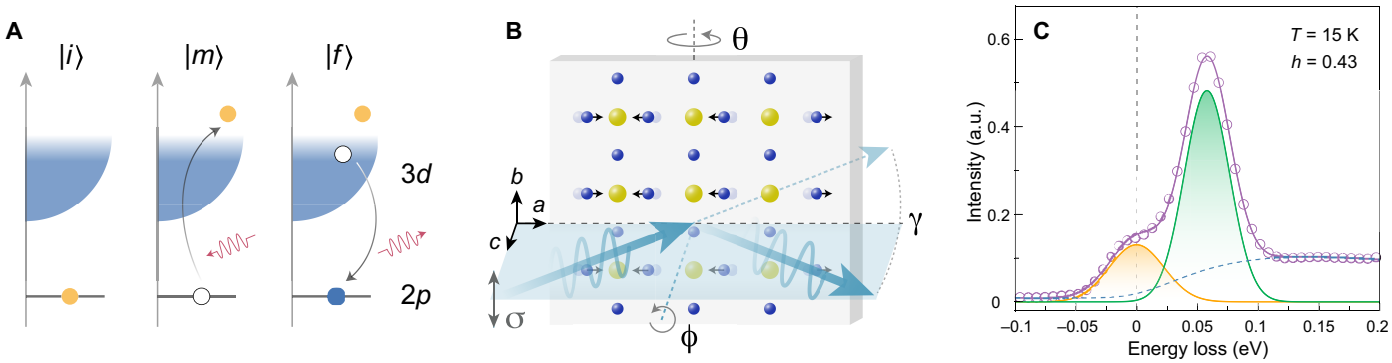

Fig. 1. Phonon excitations generated in a RIXS process. (**A**) Schematic of a two-step Cu L_3 edge RIXS process. The transition from initial $|i\rangle$ to the intermediate state $|m\rangle$ occurs upon absorption of an incident photon; a Cu 2*p* core electron is promoted to the 3*d* valence band. While the core hole is screened, the excited electron effectively causes the vibrations of the oxygen ions. A decay process leaves behind a phonon in the final state $|f\rangle$ with probability depending on the EPC (*24*). (**B**) Schematic of the scattering geometry and the eigenvector for phonons with $\mathbf{Q} = (0.25, 0, 0)$. The yellow and blue "balls" represent copper and oxygen ions, respectively. Black arrows on the oxygen ions indicate the vibration directions. (**C**) A representative RIXS spectrum collected at 15 K on LESCO. The orange solid, green solid, and blue dashed lines represent scattering from elastic, phonon, and background contributions, respectively. The fitting components are described in the main text. a.u., arbitrary units.

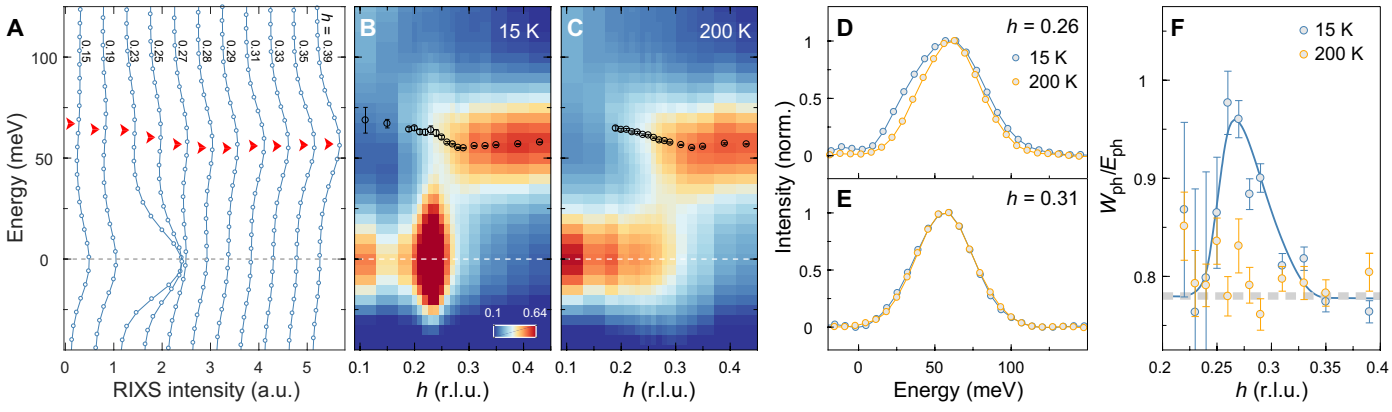

Fig. 2. Bond-stretching phonon mode in LESCO probed by RIXS. (**A**) Raw RIXS spectra collected at 15 K across the charge ordering wave vector. (**B** and **C**) RIXS intensity maps as a function of energy loss and *h* for temperatures as indicated. The red arrows in (A) and black open circles in (B) and (C) mark the phonon dispersion determined from fitting the spectra (see the main text). Color code indicates the RIXS intensity. To avoid the overwhelming elastic scattering at the charge ordering wave vector, we here present data taken along $\mathbf{Q} = (h, h \tan\varphi)$ with $\varphi = 4°$ and 0° for $T = 15$ and 200 K, respectively. r.l.u., reciprocal lattice units. (**D** and **E**) Elastic scattering and background subtracted spectra for $h = 0.26$ and 0.31. (**F**) Dimensionless parameter W_{ph}/E_{ph} as a function of *h* at 15 and 200 K. Solid lines are guides to the eye. Error bars, throughout the article, reflect SDs of the fits described in the main text.

in agreement with previous INS (*28*), IXS (*29*), and RIXS studies (*21*, *22*). As shown later, the overall dispersion and intensity also match those expected for the bond-stretching phonon. To determine its dispersion, RIXS spectra are collected as a function of momentum (Fig. 2A and fig. S2). The resulting RIXS intensity maps are shown for low (15 K) and high (200 K) temperatures in Fig. 2 (B and C). Stripe order, revealed by the reflection at $\mathbf{Q}_{CDW} = (\delta, 0)$ with $\delta \approx 0.24$, weakens by about two orders of magnitude across this temperature range [see Fig. 3F and (*30*)].

To analyze the RIXS spectra, our fitting model consists of the following three components. Elastic scattering and the bond-stretching phonon are described by Gaussian profiles. The paramagnon-dominated background, at high energy, is mimicked using a damped harmonic oscillator function convoluted with the instrumental resolution (see Fig. 1C). In Fig. 2 (D and E), subtraction of elastic and background responses isolates the bond-stretching phonon spectral weight.

In this fashion, phonon dispersion $E_{ph}(\mathbf{Q})$, lifetime effects, and EPC are studied as a function of temperature and momentum across the charge ordering wave vector $\mathbf{Q}_{CDW}$. Starting at high temperature (T = 200 K), the phonon linewidth W_{ph} is resolution-limited, and the dimensionless parameter $W_{ph}/E_{ph}(\mathbf{Q})$ is essentially featureless across $\mathbf{Q} = \mathbf{Q}_{CDW}$ (Fig. 2F). At our base temperature (15 K), the phonon linewidth undergoes a weak but statistically significant enhancement beyond the resolution near $\mathbf{Q}_{CDW}$, which indicates a decrease in the phonon lifetime. Combined with a softening of the phonon dispersion, $W_{ph}/E_{ph}(\mathbf{Q})$ displays a 20% increase across $\mathbf{Q}_{CDW}$. Although current RIXS energy resolution barely resolves the phonon lifetime, the EPC can be analyzed through the softening of the dispersion and the RIXS phonon cross section.

Density functional theory (DFT) calculations (*31*, *32*) yield a bond-stretching phonon mode that disperses weakly downward from the zone center to the boundary (see gray dashed lines in Fig. 3, A and C).

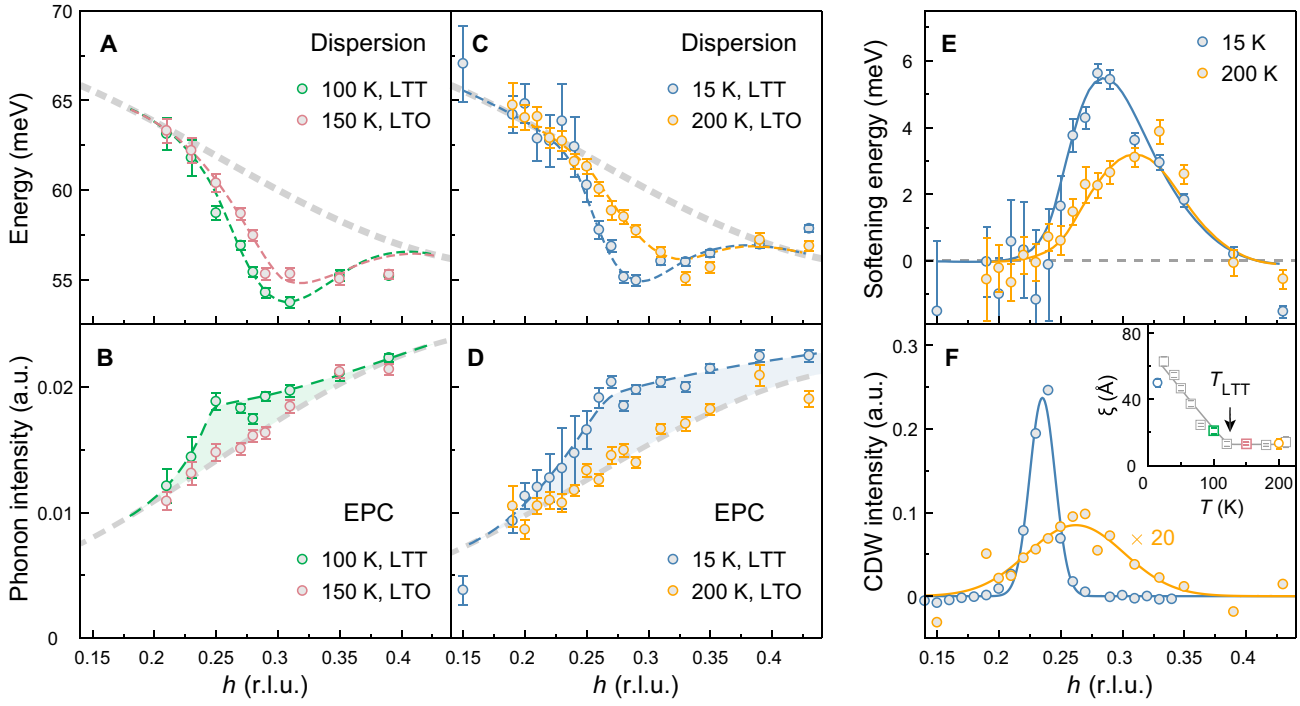

Fig. 3. Temperature evolution of charge order and the associated phonon anomaly in LESCO. (**A** and **C**) Phonon dispersions and (**B** and **D**) integrated spectral weights along the longitudinal direction at indicated temperatures. (**E**) Softening energy as a function of *h* obtained from data in (C) as described in the main text. (**F**) Charge ordering peak at 15 and 200 K. Elastic intensities are integrated over −45 to 30 meV, and the 200 K data are displayed with a multiplication factor of 20. Solid lines are Gaussian fits. The inset displays the charge order correlation length ξ versus temperature. Open squares denote data from (*30*). Gray dashed lines in (A) and (C) and in (B) and (D) are respectively the DFT bare bond-stretching phonon dispersion (normalized to match our data) and the phonon spectral weight above T_{LTT} fitted to a $\sin^2(\pi h)$ function. Colored lines in (A) to (E) are guides to the eye. LTO, low-temperature orthorhombic.

The phonon softening observed around the charge ordering wave vector is not captured by the DFT formalism. By subtracting the bare phonon dispersion from the measured data (see the Supplementary Materials for details), we infer the softening magnitude (Fig. 3E). The maximum value ~5 meV at 15 K is in good agreement with previous INS results on La-based compounds (*10*, *33*).

In contrast to INS and IXS, the phonon intensities probed by RIXS are directly proportional to the EPC (*16*, *23*–*27*). Above the LTT onset temperature ($T_{LTT} \approx 125$ K), the phonon integrated spectral weight increases monotonically with momentum $\mathbf{Q} = (h, 0)$ (Fig. 3, B and D). Upon cooling into the LTT phase, the phonon weight is enhanced in vicinity to $\mathbf{Q}_{CDW}$ (Fig. 3B). This effect is further enhanced when cooling to base temperature (Fig. 3D). Our main finding is thus that EPC, linked to the charge ordering, is amplified within the LTT phase (see Fig. 4).

DISCUSSION

The phonon softening manifests over a broad momentum range (h = 0.24 to 0.4) (Fig. 3, A and C). This is in contrast to a conventional Kohn anomaly with a sharp phonon dispersion dip and is thus incompatible with a CDW state arising from Fermi surface nesting (*8*, *10*, *34*). Alternatively, phonon anomalies in cuprates have been discussed in the context of collective stripe fluctuations (*35*, *36*). Phase excitations of stripes couple to the lattice and create a splitting of the in-phase and out-of-phase oscillation modes (*35*). However, the phonon anomaly is expected (*35*) to exist within a narrow

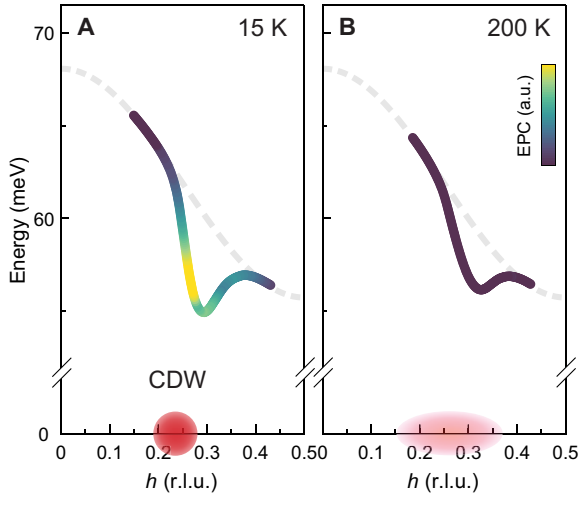

Fig. 4. Schematic temperature evolution of the charge order and EPC to the bond-stretching mode. (**A**) Low-temperature and (**B**) high-temperature charge ordering wave vector and soft bond-stretching phonon mode as observed in LESCO. Red and pink area centered around the CDW ordering wave vector schematically indicate the CDW peak width. Solid and dashed lines represent the experimentally observed and DFT-calculated bond-stretching phonon dispersions, respectively. Color code on the phonon dispersion indicates the observed EPC in addition to the expected $\sin^2(\pi h)$ dependence.

range of **Q**—at odds with our experimental observations. Another notable effect of charge excitation is its Fano interference with intersecting optical phonons. Recent RIXS results on Bi-based cuprates $Bi_2Sr_2CaCu_2O_{8+\delta}$ and $Bi_2Sr_2LaCuO_{6+\delta}$ are interpreted in terms of a Fano resonance between dispersive charge excitations and optical phonon modes (*17*, *19*, *20*). This is supported by a nonmonotonically increasing phonon intensity versus momentum and an excitation energy softening that exceeds expectations for EPC. By contrast, the here reported softening magnitude in LESCO is consistent with typical phononic self-energy effects (*10*, *33*). In addition, the intensity enhancement in the Bi-based compounds is more intense and leads to a dome-shaped *h* dependence (*17*, *19*, *20*), whereas in LESCO, the enhanced intensity is still smaller compared to that near the zone boundary (Fig. 3D). While both mechanisms could possibly be involved, the significantly smaller softening energy and intensity increase in LESCO suggest the EPC to be the dominant mechanism underlying the observed phonon anomaly. The different behaviors observed in LESCO and Bi-based compounds could be rooted in the charge ordering strength. Shorter correlation length found in Bi-based compounds makes quantum fluctuations correspondingly more relevant (*19*, *20*). Note that the enhanced phonon intensity in both the Bi-based compounds and LESCO peaks at a larger wave vector compared to $\mathbf{Q}_{CDW}$ (Fig. 3, D and F). In the former case, this is explained by the dispersive feature of intersecting charge excitations. In LESCO, this could arise from the combined effect of both electronic correlations and EPC, which, as a whole, defines the CDW.

Although this phonon anomaly is linked to the charge ordering phenomenon, there is no direct proportionality between charge order and phonon softening. For example, a pronounced phonon softening is observed already at 200 K in the presence of only weak charge ordering. Upon cooling, the charge order grows by roughly two orders of magnitude, whereas the phonon softening develops only marginally. The broad momentum width of the softening at all temperatures remains comparable to the short-range charge order peak above T_{LTT} (see Fig. 3, E and F). Together, these results suggest a strong coupling between fluctuating stripes and the bond-stretching phonon.

Momentum dependence of the EPC in cuprates has been the subject of many theoretical considerations (*16*, *24*–*27*). For the copper-oxygen bond-stretching mode, a $\sin^2(\pi h)$ dependence of intensity for $\mathbf{Q} = (h, 0)$ is expected in the absence of charge order (*16*, *25*–*27*). Recent RIXS studies, on different cuprate systems, have observed bond-stretching phonon intensities in good agreement with this theoretical modeling (*20*, *21*, *25*, *26*). It is also in accord with the intensities measured above T_{LTT} in LESCO (Fig. 3, B and D). This linkage between RIXS phonon intensity and EPC suggests that, upon cooling into the LTT phase, the EPC is enhanced around the CDW wave vector. This enhancement is further amplified upon cooling.

In $La_{2-x}Sr_xCuO_4$ $x = 1/8$ (LSCO), the RIXS intensity of bond-stretching phonon remains structureless at low temperature (28 K) (*21*). The lack of LTT lattice distortion in LSCO results in a mismatch between the copper-oxygen bond and the average stripe directions (*37*, *38*). This, in turn, reduces the coupling between the fluctuating stripes and the lattice vibrations that involve the in-plane copper-oxygen bonds. Our comparison of the bond-stretching phonon across the LTT transition temperature in LESCO reveals that the EPC is enhanced at the charge ordering wave vector only in the LTT phase (Fig. 3B). As a result of the enhanced coupling between lattice and charge stripes, the charge order correlation length gradually increases inside the LTT phase (inset of Fig. 3F). The link between the lattice LTT transition, electron-phonon coupling, and charge correlations suggests that electron-lattice interactions promote the charge ordering process.

The importance of EPC in cuprates has been underlined in many theoretical considerations (*16*, *25*, *27*, *39*). A phonon-based CDW mechanism can be enabled by strong correlations where the momentum space structure of the EPC is linked to the charge ordering wave vector (*39*). Although only the buckling mode was considered (*39*), the EPC of the bond-stretching mode is also known to be significant (*16*, *22*, *25*–*28*). Our experimental results reveal that charge correlations spontaneously emerge at high temperature where the EPC is not favoring charge instability at any specific momentum. The low-temperature EPC enhancement promotes the CDW formation by triggering a "lock-in" of charge modulation at a specific ordering wave vector. This is similar to the conventional phonon mechanism in CDW-susceptible materials, where the **Q**-dependent EPC induces a structure instability that has a compatible modulation with the charge density (*6*, *8*, *39*). In LESCO, the LTT distortion changes the in-plane copper-oxygen bond lengths with the same symmetry breaking tendency as the stripes. The ionic modulation could possibly enhance the coupling to the electronic degree of freedom and stabilize the charge stripes. With the above considerations, although it remains difficult to conclude whether the enhanced EPC is a cause or rather a feedback effect that promotes long-range CDW, our results reveal the strong coupling nature of the EPC, which plays a significant role cooperatively with electronic correlations for the charge ordering in this system. Future improvements of the RIXS energy resolution would enable studies of energetically lower lying phonons—for example, the buckling mode (*20*). Such studies would map out all the charge ordering relevant phonon modes and thus provide a comprehensive understanding of this phenomenon.

In summary, we use RIXS to study the self-energy effects and EPC of the bond-stretching phonon anomaly associated with the CDW order in LESCO. A substantial enhancement of the EPC is observed near the charge ordering wave vector upon entering the LTT phase. A tangible causal chain is that the LTT lattice structure enables a momentum-dependent EPC that, in turn, triggers a lock-in of the charge-stripe ordering wave vector and long-range charge correlations. Our results highlight the importance of electron-phonon interaction for the long-range CDW order in the cuprates. Revealing the substantial EPC to the bond-stretching mode also has important implications for elucidating the intensively debated role of phonons in cuprate superconductivity.

MATERIALS AND METHODS

Single crystals of LESCO, grown by the floating zone method, were studied at the I21 RIXS beamline at Diamond Light Source. All measurements were performed at the Cu L_3 resonance (~932.5 eV), using grazing exit geometry with linear vertical (σ) incident light polarization. We define wave vector **Q** at (q_x, q_y, q_z) as $(h, k, l) = (q_x a/2\pi, q_y b/2\pi, q_z c/2\pi)$ in reciprocal lattice units using pseudotetragonal notation, with $a \approx b \approx 3.79$ Å and $c \approx 13.1$ Å.

Scattering angle and energy resolution (Gaussian SD) were fixed to $\gamma = 154°$ and $\sigma_G = 19$ meV. Magnitude and direction of the in-plane momentum transfer $\mathbf{Q}_{||} = (h, h \tan \varphi)$ are controlled by the light incident angle θ and sample azimuthal angle φ, respectively (Fig. 1B). RIXS intensities were normalized to the weight of the *dd* excitations (see the Supplementary Materials for details).

SUPPLEMENTARY MATERIALS

Supplementary material for this article is available at http://advances.sciencemag.org/cgi/content/full/7/27/eabg7394/DC1

REFERENCES AND NOTES

1. B. Keimer, S. A. Kivelson, M. R. Norman, S. Uchida, J. Zaanen, From quantum matter to high-temperature superconductivity in copper oxides. *Nature* **518**, 179–186 (2015).
2. J. M. Tranquada, B. J. Sternlieb, J. D. Axe, Y. Nakamura, S. Uchida, Evidence for stripe correlations of spins and holes in copper oxide superconductors. *Nature* **375**, 561–563 (1995).
3. V. J. Emery, S. A. Kivelson, J. M. Tranquada, Stripe phases in high-temperature superconductors. *Proc. Natl. Acad. Sci. U.S.A.* **96**, 8814–8817 (1999).
4. J. Zaanen, O. Gunnarsson, Charged magnetic domain lines and the magnetism of high-T_c oxides. *Phys. Rev. B* **40**, 7391 (1989).
5. K. Machida, Magnetism in La_2CuO_4 based compounds. *Physica C* **158**, 192–196 (1989).
6. M. D. Johannes, I. I. Mazin, Fermi surface nesting and the origin of charge density waves in metals. *Phys. Rev. B* **77**, 165135 (2008).
7. F. Weber, S. Rosenkranz, J.-P. Castellan, R. Osborn, R. Hott, R. Heid, K.-P. Bohnen, T. Egami, A. H. Said, D. Reznik, Extended phonon collapse and the origin of the charge-density wave in 2*H*–$NbSe_2$. *Phys. Rev. Lett.* **107**, 107403 (2011).
8. X. Zhu, Y. Cao, J. Zhang, E. W. Plummer, J. Guo, Classification of charge density waves based on their nature. *Proc. Natl. Acad. Sci. U.S.A.* **112**, 2367–2371 (2015).
9. L. Pintschovius, Electron-phonon coupling effects explored by inelastic neutron scattering. *Phys. Status Solidi B* **242**, 30–50 (2005).
10. D. Reznik, Phonon anomalies and dynamic stripes. *Physica C* **481**, 75–92 (2012).
11. A. Damascelli, Z. Hussain, Z.-X. Shen, Angle-resolved photoemission studies of the cuprate superconductors. *Rev. Mod. Phys.* **75**, 473–541 (2003).
12. T. Cuk, D. H. Lu, X. J. Zhou, Z.-X. Shen, T. P. Devereaux, N. Nagaosa, A review of electron-phonon coupling seen in the high-T_c superconductors by angle-resolved photoemission studies (ARPES). *Phys. Status Solidi B* **242**, 11–29 (2005).
13. M. Fujita, H. Goka, K. Yamada, M. Matsuda, Competition between charge- and spin-density-wave order and superconductivity in $La_{1.875}Ba_{0.125-x}Sr_xCuO_4$. *Phys. Rev. Lett.* **88**, 167008 (2002).
14. M. Fujita, H. Goka, K. Yamada, M. Matsuda, Structural effect on the static spin and charge correlations in $La_{1.875}Ba_{0.125-x}Sr_xCuO_4$. *Phys. Rev. B* **66**, 184503 (2002).
15. A. P. Kampf, D. J. Scalapino, S. R. White, Stripe orientation in an anisotropic $t - J$ model. *Phys. Rev. B* **64**, 052509 (2001).
16. T. P. Devereaux, A. M. Shvaika, K. Wu, K. Wohlfeld, C. J. Jia, Y. Wang, B. Moritz, L. Chaix, W.-S. Lee, Z.-X. Shen, G. Ghiringhelli, L. Braicovich, Directly characterizing the relative strength and momentum dependence of electron-phonon coupling using resonant inelastic x-ray scattering. *Phys. Rev. X* **6**, 041019 (2016).
17. L. Chaix, G. Ghiringhelli, Y. Y. Peng, M. Hashimoto, B. Moritz, K. Kummer, N. B. Brookes, Y. He, S. Chen, S. Ishida, Y. Yoshida, H. Eisaki, M. Salluzzo, L. Braicovich, Z.-X. Shen, T. P. Devereaux, W.-S. Lee, Dispersive charge density wave excitations in $Bi_2Sr_2CaCu_2O_{8+\delta}$. *Nat. Phys.* **13**, 952–956 (2017).
18. H. Miao, R. Fumagalli, M. Rossi, J. Lorenzana, G. Seibold, F. Yakhou-Harris, K. Kummer, N. B. Brookes, G. D. Gu, L. Braicovich, G. Ghiringhelli, M. P. M. Dean, Formation of incommensurate charge density waves in cuprates. *Phys. Rev. X* **9**, 031042 (2019).
19. W. S. Lee, K.-J. Zhou, M. Hepting, J. Li, A. Nag, A. C. Walters, M. Garcia-Fernandez, H. C. Robarts, M. Hashimoto, H. Lu, B. Nosarzewski, D. Song, H. Eisaki, Z. X. Shen, B. Moritz, J. Zaanen, T. P. Devereaux, Spectroscopic fingerprint of charge order melting driven by quantum fluctuations in a cuprate. *Nat. Phys.* **17**, 53–57 (2021).
20. J. Li, A. Nag, J. Pelliciari, H. Robarts, A. Walters, M. Garcia-Fernandez, H. Eisaki, D. Song, H. Ding, S. Johnston, R. Comin, K.-J. Zhou, Multiorbital charge-density wave excitations and concomitant phonon anomalies in $Bi_2Sr_2LaCuO_{6+\delta}$. *Proc. Natl. Acad. Sci. U.S.A.* **117**, 16219–16225 (2020).
21. J. Q. Lin, H. Miao, D. G. Mazzone, G. D. Gu, A. Nag, A. C. Walters, M. García-Fernández, A. Barbour, J. Pelliciari, I. Jarrige, M. Oda, K. Kurosawa, N. Momono, K.-J. Zhou, V. Bisogni, X. Liu, M. P. M. Dean, Strongly correlated charge density wave in $La_{2-x}Sr_xCuO_4$ evidenced by doping-dependent phonon anomaly. *Phys. Rev. Lett.* **124**, 207005 (2020).
22. Y. Y. Peng, A. A. Husain, M. Mitrano, S. X.-L. Sun, T. A. Johnson, A. V. Zakrzewski, G. J. MacDougall, A. Barbour, I. Jarrige, V. Bisogni, P. Abbamonte, Enhanced electron-phonon coupling for charge-density-wave formation in $La_{1.8-x}Eu_{0.2}Sr_xCuO_{4+\delta}$. *Phys. Rev. Lett.* **125**, 097002 (2020).
23. L. J. P. Ament, M. van Veenendaal, T. P. Devereaux, J. P. Hill, J. van den Brink, Resonant inelastic x-ray scattering studies of elementary excitations. *Rev. Mod. Phys.* **83**, 705–767 (2011).
24. L. J. P. Ament, M. van Veenendaal, J. van den Brink, Determining the electron-phonon coupling strength from resonant inelastic x-ray scattering at transition metal L-edges. *Europhys. Lett.* **95**, 27008 (2011).
25. L. Braicovich, M. Rossi, R. Fumagalli, Y. Peng, Y. Wang, R. Arpaia, D. Betto, G. M. De Luca, D. Di Castro, K. Kummer, M. Moretti Sala, M. Pagetti, G. Balestrino, N. B. Brookes, M. Salluzzo, S. Johnston, J. van den Brink, G. Ghiringhelli, Determining the electron-phonon coupling in superconducting cuprates by resonant inelastic x-ray scattering: Methods and results on $Nd_{1+x}Ba_{2-x}Cu_3O_{7-\delta}$. *Phys. Rev. Res.* **2**, 023231 (2020).
26. M. Rossi, R. Arpaia, R. Fumagalli, M. Moretti Sala, D. Betto, K. Kummer, G. M. De Luca, J. van den Brink, M. Salluzzo, N. B. Brookes, L. Braicovich, G. Ghiringhelli, Experimental determination of momentum-resolved electron-phonon coupling. *Phys. Rev. Lett.* **123**, 027001 (2019).
27. S. Johnston, F. Vernay, B. Moritz, Z.-X. Shen, N. Nagaosa, J. Zaanen, T. P. Devereaux, Systematic study of electron-phonon coupling to oxygen modes across the cuprates. *Phys. Rev. B* **82**, 064513 (2010).
28. D. Reznik, L. Pintschovius, M. Ito, S. Iikubo, M. Sato, H. Goka, M. Fujita, K. Yamada, G. D. Gu, J. M. Tranquada, Electron-phonon coupling reflecting dynamic charge inhomogeneity in copper oxide superconductors. *Nature* **440**, 1170–1173 (2006).
29. T. Fukuda, J. Mizuki, K. Ikeuchi, K. Yamada, A. Q. R. Baron, S. Tsutsui, Doping dependence of softening in the bond-stretching phonon mode of $La_{2-x}Sr_xCuO_4$ ($0 \leq x \leq 0.29$). *Phys. Rev. B* **71**, 060501 (2005).
30. Q. Wang, M. Horio, K. von Arx, Y. Shen, D. John Mukkattukavil, Y. Sassa, O. Ivashko, C. E. Matt, S. Pyon, T. Takayama, H. Takagi, T. Kurosawa, N. Momono, M. Oda, T. Adachi, S. M. Haidar, Y. Koike, Y. Tseng, W. Zhang, J. Zhao, K. Kummer, M. Garcia-Fernandez, K.-J. Zhou, N. B. Christensen, H. M. Rønnow, T. Schmitt, J. Chang, High-temperature charge-stripe correlations in $La_{1.675}Eu_{0.2}Sr_{0.125}CuO_4$. *Phys. Rev. Lett.* **124**, 187002 (2020).
31. F. Giustino, M. L. Cohen, S. G. Louie, Small phonon contribution to the photoemission kink in the copper oxide superconductors. *Nature* **452**, 975–978 (2008).
32. C. Falter, T. Bauer, F. Schnetgöke, Modeling the electronic state of the high-T_c superconductor LaCuO: Phonon dynamics and charge response. *Phys. Rev. B* **73**, 224502 (2006).
33. T. Tejsner, A. Piovano, A. Ţuţueanu, A. T. Rømer, B. O. Wells, J.-C. Grivel, M. Boehm, L. Udby, Anomalous dispersion of longitudinal optical phonons in oxygen-doped $La_{2-x}Sr_xCuO_{4+\delta}$. *Phys. Rev. B* **101**, 100504 (2020).
34. W. Kohn, Image of the Fermi surface in the vibration spectrum of a metal. *Phys. Rev. Lett.* **2**, 393–394 (1959).
35. E. Kaneshita, M. Ichioka, K. Machida, Phonon anomalies due to collective stripe modes in high T_c cuprates. *Phys. Rev. Lett.* **88**, 115501 (2002).
36. S. R. Park, T. Fukuda, A. Hamann, D. Lamago, L. Pintschovius, M. Fujita, K. Yamada, D. Reznik, Evidence for a charge collective mode associated with superconductivity in copper oxides from neutron and x-ray scattering measurements of $La_{2-x}Sr_xCuO_4$. *Phys. Rev. B* **89**, 020506 (2014).
37. H. Kimura, H. Matsushita, K. Hirota, Y. Endoh, K. Yamada, G. Shirane, Y. S. Lee, M. A. Kastner, R. J. Birgeneau, Incommensurate geometry of the elastic magnetic peaks in superconducting $La_{1.88}Sr_{0.12}CuO_4$. *Phys. Rev. B* **61**, 14366 (2000).
38. V. Thampy, M. P. M. Dean, N. B. Christensen, L. Steinke, Z. Islam, M. Oda, M. Ido, N. Momono, S. B. Wilkins, J. P. Hill, Rotated stripe order and its competition with superconductivity in $La_{1.88}Sr_{0.12}CuO_4$. *Phys. Rev. B* **90**, 100510 (2014).
39. S. Banerjee, W. A. Atkinson, A. P. Kampf, Emergent charge order from correlated electron-phonon physics in cuprates. *Commun. Phys.* **3**, 161 (2020).
40. D. Reznik, T. Fukuda, D. Lamago, A. Q. R. Baron, S. Tsutsui, M. Fujita, K. Yamada, **q**-dependence of the giant bond-stretching phonon anomaly in the stripe compound $La_{1.48}Nd_{0.4}Sr_{0.12}CuO_4$ measured by IXS. *J. Phys. Chem. Solids* **69**, 3103–3107 (2008).

Acknowledgments: Q.W. and J.C. thank Z. Li, S. G. Louie, and Y. Peng for insightful discussions. We acknowledge Diamond Light Source for time on Beamline I21 under proposal MM24481. **Funding:** Q.W., K.v.A., M.H., T.S., and J.C. acknowledge support from the Swiss National Science Foundation through grant numbers BSSGI0-155873 and 200021-188564. Y.S. thanks the Chalmers Area of Advances-Materials Science and the Swedish Research Council (VR) with the starting grant (Dnr. 2017-05078) for funding. **Author contributions:** Q.W. and J.C. conceived the project. S.P., T.T., and H.T. grew the LESCO single crystals. Q.W., K.v.A., M.H., D.J.M., Y.S., T.S., A.N., M.G.-F., K.-J.Z., and J.C. performed the RIXS experiments. Q.W., K.v.A., J.K., and J.C. analyzed the data. Q.W. and J.C. wrote the manuscript with input from all authors. **Competing interests:** The authors declare that they have no competing interests. **Data and materials availability:** All data needed to evaluate the conclusions in the paper are present in the paper and/or the Supplementary Materials.

Submitted 25 January 2021
Accepted 17 May 2021
Published 30 June 2021
10.1126/sciadv.abg7394

Citation: Q. Wang, K. von Arx, M. Horio, D. J. Mukkattukavil, J. Küspert, Y. Sassa, T. Schmitt, A. Nag, S. Pyon, T. Takayama, H. Takagi, M. Garcia-Fernandez, K.-J. Zhou, J. Chang, Charge order lock-in by electron-phonon coupling in $La_{1.675}Eu_{0.2}Sr_{0.125}CuO_4$. *Sci. Adv.* **7**, eabg7394 (2021).

Science Advances

Charge order lock-in by electron-phonon coupling in $La_{1.675}Eu_{0.2}Sr_{0.125}CuO_4$

Qisi Wang, Karin von Arx, Masafumi Horio, Deepak John Mukkattukavil, Julia Küspert, Yasmine Sassa, Thorsten Schmitt, Abhishek Nag, Sunseng Pyon, Tomohiro Takayama, Hidenori Takagi, Mirian Garcia-Fernandez, Ke-Jin Zhou and Johan Chang

Sci Adv **7** (27), eabg7394.
DOI: 10.1126/sciadv.abg7394